

# Giant Saharan dust intrusion over the Southwestern Iberian Peninsula in 2022

Daniele Bortoli<sup>(a,b)</sup>, Vanda Salgueiro<sup>(b)</sup>, Maria João Costa<sup>(a,b)</sup>

<sup>a)</sup> *Department of Physics, University of Evora, 7000-671 Évora, Portugal*

<sup>b)</sup> *Institute of Earth Sciences (ICT) and Earth Remote Sensing Laboratory (EaRSLab), 7000-671 Évora, Portugal*  
*db@uevora.pt*

**Abstract:** Starting on March 15<sup>th</sup>, 2022, the Iberian Peninsula, as well as Central Europe, were affected by the transport of Saharan desert dust originating from North Africa. Despite being a relatively frequent phenomenon at this time of year, this intrusion was the most intense since there are records in the European network EARLINET for this site. The transport of particles from the Sahara Desert was monitored at the Evora Atmospheric Sciences Observatory (EVASO) at the Institute of Earth Sciences (ICT), at the University of Évora.

The plume was transported at low altitude, being detected at the surface, in Évora, on the morning of March 15<sup>th</sup>, 2022, persisting over the city until late morning of March 17<sup>th</sup>. The air quality index during this period was classified as poor, indicating the most serious level of pollution. The effect of these particles was visible to the naked eye, manifesting in the color and opacity given to the sky, deposition on surfaces, “mud rain” and notably vibrant sunrises and sunsets.

## 1. Introduction

Atmospheric particles, commonly known as aerosols, originate from both natural sources and human activities, and they wield significant influence across a wide spectrum of atmospheric processes, impacting the Earth's climate system on various temporal and spatial scales. These particles directly affect the atmospheric radiative balance by scattering and absorption of the solar and thermal radiation, while they exert an indirect effect through their interactions with clouds, altering cloud albedo, lifetime and precipitation patterns [1-5]. Moreover, aerosols have the potential to diminish the reflective properties (albedo) of ice and snow surfaces [6,7], and they participate in atmospheric chemistry dynamics [8,9]. Conversely, depending on their concentration and composition, aerosols can adversely affect air quality and visibility, thereby posing risks to public health and safety. As stated in the latest technical report of the Intergovernmental Panel on Climate Change (IPCC2023), the meteorological extreme events are increasing in magnitude and frequency, and in this frame can be inserted the intense desert dust plume observed over all Europe during March 2022. In this work we focus on the analysis of the events over the south western region of the Iberian

Peninsula and in particular at the Evora Observatory (38.57, -7.90). The characterization of the event is conducted with a synergic use of multiple remote sensing devices to retrieve the optical properties of the particles as well as with conventional (in situ) analyzers to assess the air quality index.

## 2. Instruments and Methods

The Evora Atmospheric Sciences Observatory (EVASO) is equipped with multiple instruments. In this work, data obtained from two lidar systems are used: the Vaisala Ceilometer mod. CL31 [10] and the Portable Aerosol and cLOUD Lidar (PAOLI), a multi-wavelength Raman lidar PollyXT system [11]. Also, data from the Beta Gauge monitor mod. MP401 by Environnements [12] and the amazing images obtained with the sky camera will be shown.

The CL31 instrument provides the Attenuated back scattered signals with a very high temporal and spatial vertical resolution resolutions of 10 s and 10 m respectively. These resolutions need to be averaged to obtain a higher SNR. The CL31 is part of the E-Profile network ([www.e-profile.eu](http://www.e-profile.eu)).

The PAOLI instrument provides observations of backscattered radiation profiles with vertical

and temporal resolutions of 30 m and 30 s, respectively. The lidar overlap affects the lowest 800 m. From the optical measurements, the particle extinction coefficients and particle linear depolarization profiles are retrieved with the Single Calculus Chain (SCC) tool [13]. During day-time only the elastic lidar signals at 355, 532 and 1064 nm are used due to strong daylight background and the Fernald-Klett method is employed for the determination of the particle backscatter coefficient profiles. During night-time period, the particle backscatter and extinction coefficient profiles are determined from the inelastic lidar signal using the Raman lidar method. The particle linear depolarization ratio ( $\delta_p$ ) at 532 nm is also retrieved during both day-time and night-time periods. PAOLI is a member of the EARLINET network ([www.earlinet.org](http://www.earlinet.org)).

The MP101 analyzer measures concentration of suspended particulate matter with diameter less than 10  $\mu\text{m}$ . The measurement principle is based on the attenuation of the beta radiation reaching the Geiger-Muller counter due to the particles deposited on the glass fibre filter. The samplings are carried out at scheduled intervals with a vacuum pump through the sampling head connected to the analyzer. The amount of radiation reaching the detector is decreased as the mass of the particulate spot increases. This method has the advantages of non-destructive physical measurement and fast automated operation, both of which are desirable when dealing with large amounts of data requirement. The beta attenuation method gives the possibility to have results in near real time without the necessity to interrupt the measurement cycle. The MP101 at EVASO is also equipped with an optical module that allows for the measurements of PM<sub>2.5</sub> and PM<sub>1</sub> concentrations, through the attenuation of an infrared laser beam.

The all sky camera is based on the P1343 surveillance camera by AXIS coupled with a NIKON fisheye with a Field of View of 183°. The embedded linux OS allows for the capture of images at predefined intervals of 5 minutes. In addition the image post processing yields the cloud cover evolution.

### 3. Observations and Results

The events started on the morning of March 15<sup>th</sup> at an altitude of about 5 km as detected by the CL31 ceilometer (Figure 1).

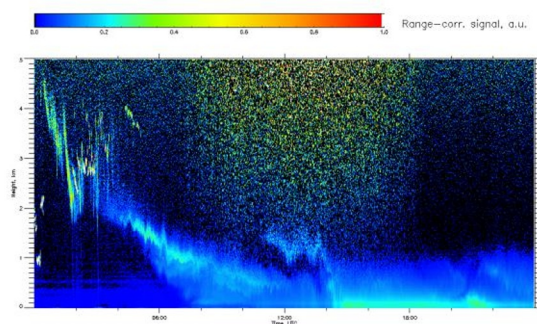


Figure 1. CL31 attenuated backscattered profiles on 15 March 2022.

The same features can be seen in the range corrected signal plot of the PAOLI observations (figure 2)

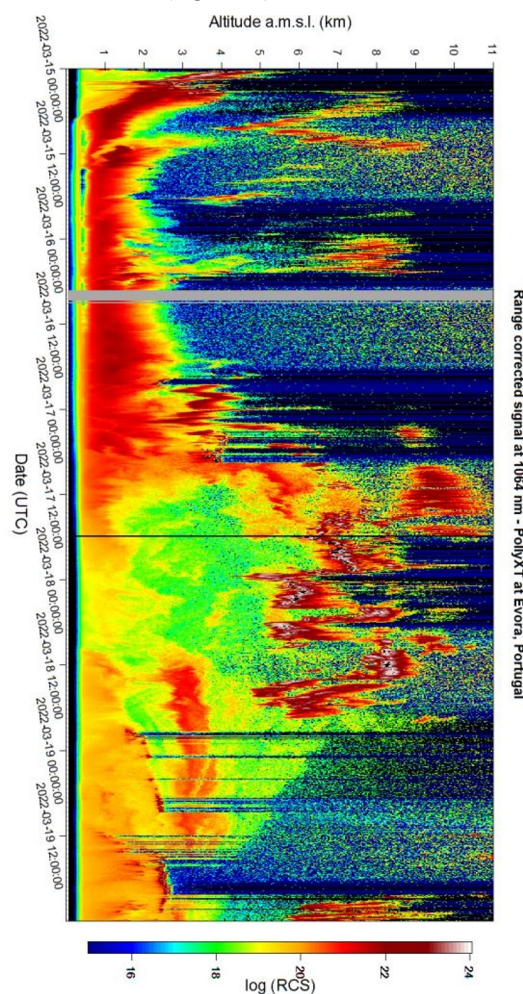


Figure 2. PAOLI Range corrected signal for the infrared channel during 15-19 March 2022.

It can be seen that the event lasted for almost 1 week even if the ‘giant’ loading at the surface occurred on 15-16 of March.

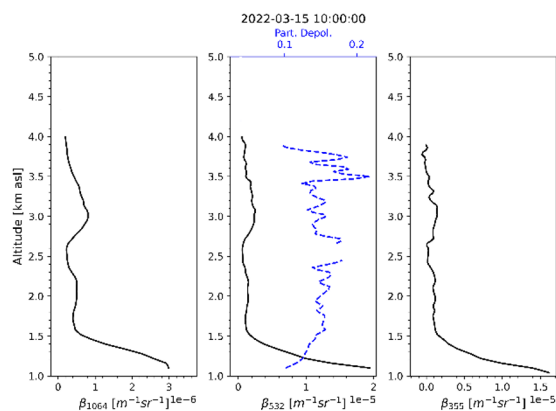


Figure 3. Backscatter profiles on 15 March 2022, from 10:00 to 10:30 UTC.

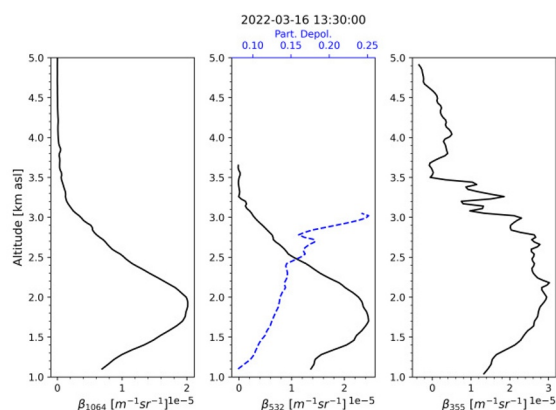


Figure 4. Backscatter profiles on 16 March 2022, from 13:30 to 14:00 UTC.

The European Air Quality Directive defines a daily average limit value for PM10 of  $50 \mu\text{g}/\text{m}^3$ , and this value cannot be exceeded more than 35 times during the year. When this value is exceeded, it may pose some risks to public health, and in these cases the population must adopt protective measures. As shown in figure 5 in Evora on 15 of March, the maximum concentration value of  $784 \mu\text{g}/\text{m}^3$  has been measured at 19:37 as reported by the MP101 particle analyzer. The calculated daily average was of  $424 \mu\text{g}/\text{m}^3$  exceeding limit value of almost an order of magnitude. Interesting to note that the PM10 maximum concentration values (over  $400 \mu\text{g}/\text{m}^3$ ) correspond PM2.5 values lower of about 40%, while with PM10 concentration under the  $400 \mu\text{g}/\text{m}^3$  the difference with the PM2.5 concentration range

from 5 to 15%. The air quality index on 15 of March has been classified as bad, the most serious level of pollution. Measurements carried out at the Institute of Earth Sciences indicate that a maximum of  $784 \mu\text{g}/\text{m}^3$  was reached yesterday in Évora at 19:37 and an average value in the last 24 h of  $424 \mu\text{g}/\text{m}^3$  (the legislation defines a daily limit of PM10 of  $50 \mu\text{g}/\text{m}^3$ ).

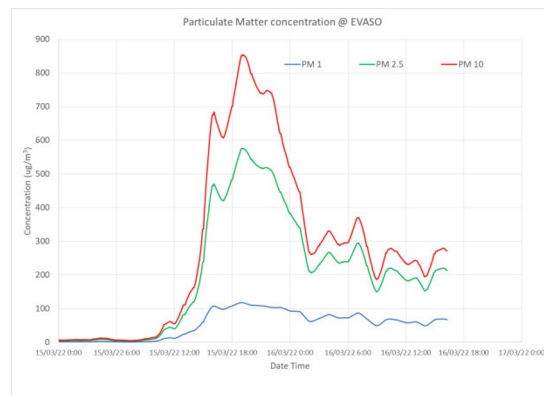


Figure 5. Particle concentration from 15 to 17 March 2022 measured with the Beta Gauge monitor

The visibility during the event was clearly worse than during the typical day in Evora. In the images obtained with the All-sky camera reported in Figure 6, the difference between different sky conditions: mixture of desert dust in presence of clouds (Left), pure desert dust without clouds (Right) and typical cloudless and dust free case (Bottom).



Figure 6. Images obtained with the Skycam at EVASO on 15 March at 10:30 UTC (Left) and on 16 March at 13:30 UTC (Right). Typical clear sky in Evora (Bottom)

#### 4. References

[1] Andreae, M.O., Rosenfeld, D., Aerosol-cloud-precipitation interactions. Part 1. The nature and

sources of cloud-active aerosols. *Earth-Science Reviews* 89, 13–41, (2008).

[2] Boucher, O., Randall, D., Artaxo, P., Bretherton, C., Feingold, G., Forster, P., Kerminen, V.-M., Kondo, Y., Liao, H., Lohmann, U., Rasch, P., Satheesh, S.K., Sherwood, S., Stevens, B., Zhang, X.Y., 2013. Clouds and aerosols, Clouds and Aerosols. In: *Climate Change 2013: The Physical Science Basis. Contribution of Working Group I to the Fifth Assessment Report of the Intergovernmental Panel on Climate Change*. Cambridge university Press, Cambridge, United Kingdom and New York, NY, USA.;

[3] Feingold, G., Eberhard, W.L., Veron, D.E., Previdi, M., First measurements of the Twomey indirect effect using ground-based remote sensors. *Geophysical Research Letters* 30, 19–22,(2003);

[4] Haywood, J., Boucher, O., Estimates of the direct and indirect radiative forcing due to tropospheric aerosols: A review. *Reviews of Geophysics* 38, 513–543, (2000).;

[5] Rosenfeld, D., Andreae, M.O., Asmi, A., Chin, M., de Leeuw, G., Donovan, D.P., Kahn, R., Kinne, S., Kivekäs, N., Kulmala, M., Lau, W., Schmidt, K.S., Suni, T., Wagner, T., Wild, M., Quaas, J., Global observations of aerosol-cloud-precipitation-climate interactions. *Reviews of Geophysics* 52, 750–808, (2014).

[6] Lisok, J., Rozwadowska, A., Pedersen, J. G., Markowicz, K. M., Ritter, C., Kaminski, J. W., Struzewska, J., Mazzola, M., Udisti, R., Becagli, S., and Gorecka, I.: Radiative impact of an extreme Arctic biomass-burning event, *ACP.*, 18, 8829–8848, (2018).

[7] Stohl, A., Andrews, E., Burkhart, J.F., Forster, C., Herber, A., Hoch, S.W., Kowal, D., Lunder, C., Mefford, T., Ogren, J.A., Sharma, S., Spichtinger, N., Stebel, K., Stone, R., Ström, J., Tørseth, K., Wehrli, C., Yttri, K.E., Pan-Arctic enhancements of light absorbing aerosol concentrations due to North American boreal forest fires during summer 2004. *JGR Atmospheres* 111, 1–20, (2006).

[8] Carslaw, K.S., Boucher, O., Spracklen, D. V., Mann, G.W., L. Rae, J.G., Woodward, S., Kulmala, M., A review of natural aerosol interactions and feedbacks within the Earth system. *ACP* 10, 1701–1737, (2010);

[9] Keywood, M., Kanakidou, M., Stohl, A., Dentener, F., Grassi, G., Meyer, C.P., Torseth, K., Edwards, D., Thompson, A.M., Lohmann, U., Burrows, J., Fire in the air: Biomass burning impacts in a changing climate. *Critical Reviews in Environmental Science and Technology* 43, 40–83, (2013).

[10] Kotthaus, S., O'Connor, E., Münkel, C., Charlton-Perez, C., Haefelin, M., Gabey, A. M., and Grimmond, C. S. B.: Recommendations for processing atmospheric attenuated backscatter

profiles from Vaisala CL31 ceilometers, *Atmos. Meas. Tech.*, 9, 3769–3791 (2016)

[11] Althausen, D., Engelmann, R., Baars, H., Heese, B., Ansmann, A., Müller, D., Komppula, M., Portable raman lidar pollyxt for automated profiling of aerosol backscatter, extinction, and depolarization. *Journal of Atmospheric and Oceanic Technology* 26, 2366–2378. (2009)

[12] Shukla, K., Aggarwal, S.G., A Technical Overview on Beta-Attenuation Method for the Monitoring of Particulate Matter in Ambient Air. *Aerosol Air Qual. Res.* 22, 220195 (2022)

[13] D'Amico, G., Amodeo, A., Mattis, I., Freudenthaler, V., Pappalardo, G., 2016. EARLINET Single Calculus Chain-technical andndash; Part 1: Pre-processing of raw lidar data. *Atmospheric Measurement Techniques* 9, 491–507. (2016)